Journal of Molecular Catalysis B: Enzymatic 61 (2009) 129–135

Contents lists available at ScienceDirect

Journal of Molecular Catalysis B: Enzymatic

journal homepage: www.elsevier.com/locate/molcatb

Enzymatic synthesis and 3-D structure of anti-proliferative acidic (MeGlcUA) xylotetrasaccharide

Annabella Tramice[a], Dominique Melck[a], Ada Virno[b], Antonio Randazzo[b], Andrea Motta[a], Antonio Trincone[a,*]

[a] Istituto di Chimica Biomolecolare, Consiglio Nazionale delle Ricerche, Via Campi Flegrei 34, 80072 Pozzuoli, Napoli, Italy
[b] Dipartimento di Chimica delle Sostanze Naturali, Università di Napoli Federico II, Via D. Montesano 49, 80131 Napoli, Italy

ARTICLE INFO

Article history:
Received 13 January 2009
Received in revised form 29 April 2009
Accepted 11 May 2009
Available online 18 May 2009

Keywords:
Enzymatic synthesis
Transglycosylation
Acidic xylosides
3-D structure

ABSTRACT

Anomerically free acidic xylo-oligosaccharides have shown interesting biological properties when tested against Gram-positive and Gram-negative aerobically grown bacteria, as well as against *Helicobacter pylori*, sarcoma-180 and other tumors. We report here a structure–activity relationship study on the role of 4-O-methyl glucuronic acid (MeGlcUA) in regulating aggregation of β-polyxylosides of (9H-fluoren-9-yl)- methanol obtained *via* the action of *Thermotoga neapolitana* xylanase. Neutral compounds from mono- to penta-β-1,4 xylosides were obtained from this biocatalyzed reaction. In addition, acidic components among products, carrying an α-1,2 4-O-methyl glucuronic acid (MeGlcUA) were also isolated. An anti-proliferative test of these compounds on human epithelial EFO 27 ovarian cancer cells indicated that the presence of MeGlcUA modulates their biological activity, while its absence induces molecular aggregation. The three-dimensional structure of the most active MeGlcUA β-polyxyloside was investigated by resorting to NOESY experiments supported by dynamic force-field calculations with/without constraints. The 3D structure is characterized by all sugars possessing a $^4C_1$ chair conformation. The MeGlcUA moiety, and the external and middle xyloses adopt a hairpin-shaped conformation, generating a non-planar arrangement of the molecule with the aromatic ring folding back toward the carbohydrate chain. Such a non-planar conformation may justify the lack of aggregation.

1. Introduction

The chemical synthesis of oligosaccharides is often convoluted but these important molecules can also be obtained in high yield with stereospecific construction of glycosidic bonds by resorting to glycoside hydrolases (endo- and exo-glycosidases) [1]. In particular, the biotechnological production of biologically valuable oligoxylosides, through enzymatic reactions based on naturally occurring donors such as xylan, is well known [2,3]. Strategies based on endoglycosidases include both the hydrolysis by endo-cleavage of sugar polymers and the transglycosylation reaction. In the first case, anomerically free fragments are obtained, often in mixtures, while the one-pot transfer of a preformed oligosaccharide unit (di- or higher) on a substrate acceptor, allows a relatively easy access to complex, biologically relevant glycosides of defined structure at anomeric center. It is reported that anomerically free acidic xylo-oligosaccharides display interesting biological properties. Two acidic fragments have been tested against Gram-positive and Gram-negative aerobically grown bacteria, as well as against *Helicobacter pylori* [4]; furthermore, glucuronic acid-containing (acidic) xylans have been reported to markedly inhibit the growth of sarcoma-180 and other tumors. However, some open questions such as the unequivocal relationship of activity with the 4-O-methyl-D-glucuronic acid content and distribution pattern, still remain [5,6].

(9H-fluoren-9-yl)-methanol and related glycosides are interesting molecules listed among interferon-inducing and anti-Herpes simplex virus active compounds [7]. The aglycone was found to be a useful acceptor for the synthesis of xylo-oligosides up to β-tetraxyloside using *Thermotoga neapolitana* xylanase activity [8].

The intrinsic propensity to irreversibly aggregate may compromise the bioavailability and therapeutic activity of biopharmaceuticals, increasing also the risk of immunogenic reactions [9–11]. Self-aggregation proceeds through a multistep association, and smaller assemblies (soluble oligomers often undetectable) may be even more detrimental than mature aggregates. As a result, there is an increasing search for efficient molecular tools that may help in preventing aggregation and favor drug bioavailability [12].

* Corresponding author at: Istituto di Chimica Biomolecolare, Consiglio Nazionale delle Ricerche, Comprensorio Olivetti, Edificio A, Via Campi Flegrei 34, I-80078 Pozzuoli, Napoli, Italy. Tel.: +39 081 8675095; fax: +39 081 8041770.
E-mail addresses: antonio.trincone@icb.cnr.it, atrincone@icmib.na.cnr.it (A. Trincone).

1381-1177/$ – see front matter © 2009 Elsevier B.V. All rights reserved.
doi:10.1016/j.molcatb.2009.05.005

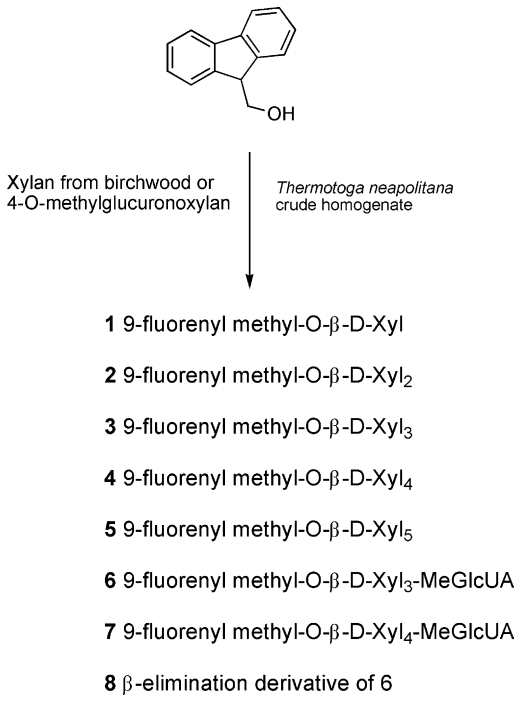

Scheme 1. Neutral and acidic xylo-oligosaccharides obtained by biocatalyzed transxylosylation reaction using *T. neapolitana* crude homogenate.

In this article the biocatalyzed production, the NMR identification and 3D structure of β-polyxylosides of (9H-fluoren-9-yl)-methanol are reported. An anti-proliferative test of these compounds on human epithelial EFO 27 ovarian cancer cells indicated that the presence of MeGlcUA modulated their biological activity, while its absence induced molecular aggregation. The three-dimensional structure of the most active MeGlcUA β-polyxyloside (**6**, Scheme 1), investigated by NMR spectroscopy and calculations, is characterized by all sugars with a $^4C_1$ chair conformation. The MeGlcUA moiety, and both xyloses, the Xyl_3 (external) and the Xyl_2 (middle) adopted a hairpin-shaped conformation generating a non-planar arrangement of the molecule with the aromatic ring folding back toward the carbohydrate chain. Such a non-planar conformation may justify the lack of aggregation.

2. Experimental

2.1. General

Reverse-phase silica gel and TLC silica gel plates were obtained from Merck (Darmstadt, Germany). Protein concentration was determined using the Bradford assay system (Bio-Rad, Hercules, CA). Compounds were visualized (TLC) under UV light or by charring with α-naphthol reagent. Chromatographic purifications were performed using MeOH/H_2O or EtOAc/MeOH gradients for Merck Lobar reverse-phase and silica-gel chromatography, respectively. EtOAc/MeOH/H_2O (70:20:10, v/v/v) was used for preparative TLC. Agilent 8453 UV–visible Spectroscopy System, Agilent Technologies, Waldbronn, Germany was used for spectrophotometric analysis. ESI-MS spectra were obtained on a Q-Tof mass spectrometer, Waters.

2.2. Biocatalysis

Growth conditions and crude homogenate preparation of *T. neapolitana* were reported elsewhere [8]. The cells were suspended in sodium phosphate buffer, pH 7.5, and disrupted by 2 passages through a French press cell. After centrifugation cell debris was removed and the soluble fraction was used as the crude homogenate (1.8 mg/mL of total protein).

The reaction using (9H-fluoren-9-yl)-methanol as acceptor was conducted in CH_3CN/100 mM Na-phosphate, pH 7.5 (13:87, v/v) containing the crude homogenate (257 μg/mL of crude protein), 20 g/L xylan from birchwood (Sigma, X0502) or 4-O-Me-glucuronoxylan (Sigma, M5144) and 0.11 M (9H-fluoren-9-yl)-methanol. After 6.5 h at 70 °C under agitation, the reaction mixture was subjected to repeated reverse-phase column chromatography (Merck Lobar RP-18) eluting with water, thus efficiently separating total chromophoric xylosylated fraction (Scheme 1) from free saccharides. Prior to acetylation, usually adopted to establish the interglycosidic linkages via NMR spectroscopy, ESI-MS spectra indicated molecular weights of native materials, thus ruling out the presence of acetyl groups possibly present in the natural xylan blocks [2] enzymatically transferred.

2.3. NMR experiments

For acquisition of NMR spectra, various concentrations of compounds were used in 100% D_2O (CortecNet, France), pH 3.7 and 6.8 (uncorrected glass-electrode readings), all in phosphate buffer. ^1H NMR spectra, acquired at the NMR Service of Istituto di Chimica Biomolecolare of CNR (Pozzuoli, Italy), were recorded at 600.13 MHz on a Bruker DRX-600 spectrometer, equipped with a TCI CryoProbe^{TM}, fitted with a gradient along the *Z*-axis. Spectra were referenced to internal sodium 3-(trimethyl-silyl)-(2,2,3,3-$^2H_4$) propionate (Aldrich, Milwaukee, WI). Total correlation spectroscopy TOCSY [13,14] and NOESY [15] spectra were recorded by using the time proportional phase incrementation of the first pulse. In general, 256 equally spaced evolution-time period t_1 values were acquired, averaging 16 transients of 2048 points, with 6024 Hz of spectral width. Time-domain data matrices were all zero-filled to 4K in both dimensions, thus yielding a digital resolution of 2.94 Hz/pt. Prior to Fourier transformation, a Lorentz-to-Gauss window with different parameters was applied for both t_1 and t_2 dimensions for all the experiments. NOESY spectra were obtained with different mixing times (50, 100, 150, 250 and 350 ms), and the recycle time was set to 5 times the longest t_1. TOCSY experiments were recorded with spin-lock periods of 64 ms, achieved with the MLEV-17 pulse sequence. Both NOESY and TOCSY experiments were performed at 300 K. Linear prediction was applied to extend the data to twice their length in t_1. The ^1H and ^{13}C natural abundance HSQC and HMBC spectra [16,17] were recorded at 300 K on the DRX-600 spectrometer, operating at 150.90 MHz for ^{13}C. 128 equally spaced evolution time period t_1 values were acquired, averaging 48 transients of 2048 points and using GARP4 for decoupling. The final data matrix was zero-filled to 4096 in both dimensions, and apodized before Fourier transformation by a shifted cosine window function in t_2 and in t_1. Linear prediction was also applied to extend the data to twice their length in t_1.

2.4. Structure calculation

Cross-peak volume integrations were performed with the program FELIX 98, using the NOESY experiment collected at mixing time of 150 ms. The NOE volumes were then converted to distance restraints after they were calibrated using known fixed distances of H5′ and H5″ of the xylose subunits. Then a NOE restraint file was generated with three distance classifications as follows: strong NOEs ($1.0\,Å \le r_{ij} \le 3.0\,Å$), medium NOEs ($2.5\,Å \le r_{ij} \le 4.5\,Å$) and weak NOEs ($4.0\,Å \le r_{ij} \le 6.0\,Å$). A total of 38 NOEs derived distance restraints were used.

Proton/proton ($^3J_{HH}$) coupling constants were measured from 1D proton spectra. Dihedral angles were calculated using the *J*-values extracted by solving the Karplus equation [18] with coefficients $A = 6.98$, $B = -1.38$, $C = 1.72$ for $^3J_{HH}$ [19]. Eleven dihedral angle constraints (that yielded only two real roots when solving Karplus equation) were used during structural calculation.

Three-dimensional structures which satisfy NOE and dihedral angle constraints were constructed by simulated annealing calculations. All calculations used a distance dependant macroscopic dielectric constant of 4r and an infinite cut-off for non-bonded interactions to partially compensate for the lack of the solvent [20]. Initial structures of the compound **6** was built using a completely random array of atoms. Using the steepest descent followed by quasi-Newton–Raphson method (VA09A) the conformational energy was minimized. Restrained simulations were carried out *in vacuo* for 12.5 ns using the CVFF force field as implemented in Discover software (Accelrys, San Diego, CA). Then, the temperature was decreased stepwise from 1000 to 250 K. The final step was again to energy-minimize to refine the structures obtained, using successively the steepest descent and the quasi-Newton–Raphson (VA09A) algorithms. Both dynamic and mechanic calculations were carried out by using a 1 (kcal/mol)/Å^2 flatwell restraints. A total of 50 structures were generated. Illustrations of structures were generated using the INSIGHT II program, version '98 (Accelrys, San Diego, CA). All the calculations were performed on a PC running Linux WS 4.0.

To account for the inherent flexibility of the molecule, unrestrained MM was also used to avoid biasing of the structure based on NOE data deriving from multiple conformational equilibria [21].

2.5. Cell proliferation assay

Human ovary adenocarcinoma (EFO 27) cell lines (DSMZ, Braunschweig, Germany) were cultured in RPMI 1640 medium containing 20% fetal bovine serum, 2 mM L-glutamine, 1× MEN non-essential amino-acids and 1 mM sodium pyruvate. Cell proliferation assays were carried out in duplicate in 6-well dishes containing cells at a density of 5×10^4 cells/well, and were incubated at 37 °C in a humidified atmosphere containing 5% CO_2. Four hours after cell seeding, vehicle (DMSO) or compounds at different concentrations were added to the medium, and thereafter daily at each change of medium for 4 days. The effect of compounds on cell growth was measured by crystal violet staining. After staining, cells were lysated in 0.01% acetic acid and analyzed by spectrophotometric analysis at $\lambda = 595$ nm. Optical density values of vehicle-treated cells (control) was considered as 100% of proliferation. The survival rate was calculated from the following formula: % survival = absorbance of drug treated/absorbance of control × 100. The percentage survival was used to evaluate the sensitivity of tumor cells.

3. Results and discussion

3.1. Enzymatic glycosylation, structural characterization and resonance assignments

In the presence of the acceptor (9H-fluoren-9-yl)-methanol, the crude homogenate of *T. neapolitana* yielded interesting transxylosylation products [8].

The reaction for the enzymatic synthesis of xylosides reported here was conducted in the presence of 13% acetonitrile necessary to dissolve 0.1 M aglycone, relying on the unusual resistance of the thermophilic enzyme, and two different xylan polymers. Using xylan from birchwood we obtained, 192 mg of total xylosides per gram of xylan used (74% neutral xylosides and 26% acidic components). Using 4-O-Me-glucuronoxylan the total yield was 84 mg per gram of xylan used (70% neutral xylosides and 30% acidic components). Neutral compounds **1**–**5** (Scheme 1), from mono- to penta-β-1,4 xylosides were obtained in yield 52.2, 23.8, 30.9, 24.5 and 10.9 mg/g of birchwood xylan used, respectively. The acidic components among products were also isolated (Scheme 1): **6**, 20 mg/g birchwood xylan; **7**, 14.6 mg/g birchwood xylan, and an additional unsaturated xylosides **8** in yield of 10 mg/g birchwood xylan. An additional non-separable mixture of minor compounds (4.8 mg/g birchwood xylan), was also obtained.

Data for compounds **1**–**4** (Scheme 1) previously reported [8], and NMR results reported here for **5**–**8** (Scheme 1) have demonstrated the purity of each product with respect to β-1,4 interglycosidic linkages as present in the natural polymers used.

The structure of compound **5** (Scheme 1) was established by mass (*m*/*z* 879 [M+Na]$^+$) and ^{1}H NMR spectra; in the latter, five anomeric signals were observed in CD_3OD at 4.42, 4.37 (× 3H), and 4.35 ppm which in an HSQC experiment correlated with carbon signals at 104.10 and 103.20 ppm. The remaining signals, in comparison to those found for compounds **1**–**4**, were in accord with the structure proposed.

The ^{1}H NMR spectrum of compound **6** (*m*/*z* 828, [M+2Na]$^+$) is reported in Fig. 1. Spin systems were identified by COSY, TOCSY and HSQC experiments recorded in D_2O (Table 1). Positioning of acidic residue was achieved by evaluating long-range correlations in HMBC experiments; we started by searching for the anomeric signal (H/C, 4.40/104.00 ppm) of xylopyranose bound to aglycon (Xyl_1). The proton signal showed long-range correlation with hydroxymethylene carbon atom of (9H-fluoren-9-yl)-methanol at 72.24 ppm and its methine carbon at 49.18 ppm. Conversely, anomeric carbon at 104.00 ppm correlated with 4.34, 4.14 (aglycon methylene protons) and 4.29 (methine proton). Furthermore, a correlation of the aromatic C1′ at 145.30 ppm with the anomeric proton at 4.40 ppm was also clearly visible. COSY- and TOCSY-correlated H4/C4 of Xyl_1 unit (3.72/77.40 ppm), showed clear long-range correlations to the anomeric proton/carbon atom of the second xylopyranose unit Xyl_2 (4.43/102.52 ppm). In similar manner the β-1,4 interconnection to the Xyl_3 moiety was also established, in fact C4 of Xyl_2 (77.05 ppm) correlated with anomeric proton of Xyl_3 at 4.59 ppm. The α-1,2 interglycosidic linkage of 4-O-methyl glucuronic with Xyl_3 unit was clearly evidenced by correlation of xylopyranose H2 proton at 3.41 ppm with anomeric carbon atom of 4-O-MeGlcUA at 98.42 ppm. A *ca.* 3 ppm low-field glycosylation

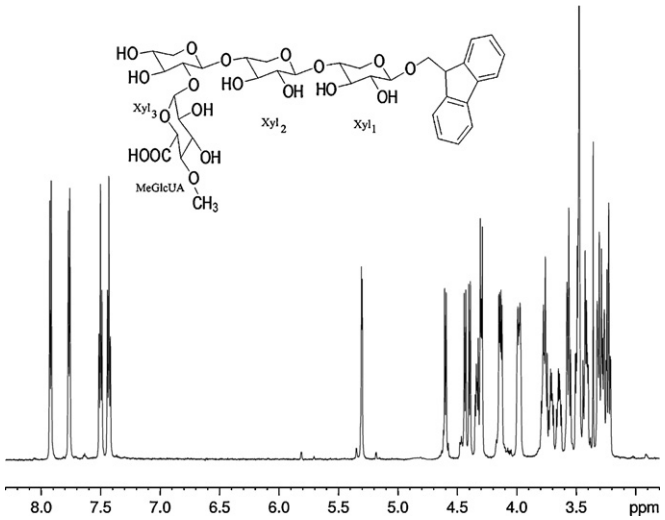

Fig. 1. ^{1}H NMR spectra of compound **6** at 4.9 mM (see insert for structure and Table 1 for signal assignments).

Table 1
NMR chemical shifts (ppm) of compound **6** in ^2H_2O.

Positions[a]	1	2	3	4	5	5′	COOH	OMe
MeGlcUA-Xyl$_3$-Xyl$_2$-**Xyl$_1$**-9FM	4.40 104.00	3.24 74.51	3.49 75.32	3.72 77.40	3.99 63.80	3.29 63.80	–	–
MeGlcUA-Xyl$_3$-**Xyl$_2$**-Xyl$_1$-9FM	4.43 102.52	3.26 74.61	3.56 73.63	3.77 77.05	4.13 63.71	3.43 63.71	–	–
MeGlcUA-**Xyl$_3$**-Xyl$_2$-Xyl$_1$-9FM	4.59 102.50	3.41 77.44	3.50 73.20	3.65 70.41	3.97 65.94	3.31 65.94	–	–
MeGlcUA-Xyl$_3$-Xyl$_2$-Xyl$_1$-9FM	5.30 98.42	3.57 72.31	3.76 73.20	3.22 83.40	4.30 73.60	– –	– 177.61	3.47 60.70
9FM	1′ – 145.30	2′ 7.92 121.10	3′ 7.43 128.33	4′ 7.46 128.80	5′ 7.76 126.10	6′ – 141.90	CH– 4.29 49.18	CH_2– 4.34–4.14 72.24

[a] Chemical shifts refer to residues in bold; for structure see Fig. 1.

shift of C2 of xylopyranose unit (77.40 ppm) was also observed by comparison with other C2 signals of the molecule. As far as position of methoxyl group of glucuronic acid moiety is concerned, it was established by multiple long-range correlations observed for position 4 of residue; this H4 (3.22 ppm) correlates with methyl carbon (60.70 ppm) and methyl protons correlate with C4 position (83.40 ppm). Remaining signals of sugars, and aglycon moiety were easily assigned, and are reported in Table 1.

The knowledge of precise value of H4/C4 of MeGlcUA was particularly interesting for structural assignment of compound **8** (Scheme 1), the β-elimination derivative of **6**, in which a methanol molecule was lost with C5–C4 double bond formation. Hexenuronic acid thus formed is a known β-elimination product of 4-O-MeGlcUA [22]. Compound **8** indeed, is characterized by the presence in the ^{1}H NMR spectrum of a doublet signal at 5.68 ppm (J = 3.51 Hz) correlating with a ^{13}C signal at 107.91 ppm. Both of them, with the absence of 3.47/60.70 signals typical of the 4-O-methyl group, are diagnostic for the presence of 4-deoxy hexenuronic acid in the molecule. The remaining signals of compound **8** in both ^{13}C and ^{1}H NMR spectra, with ESI-MS information (m/z 795 [M-H+2Na]$^+$), firmly established the structure proposed for this compound as the 4-deoxy hexenuronic acid derivative of **6**.

Mass spectra of compound **7** indicated an additional xylose unit in the molecule (m/z 960 [M+2Na]$^+$) with respect to **6**. Extensive spectroscopic NMR study confirmed its structure after a comparison with data of compound **6**. 4-O-MeGlcUA positioned on the Xyl$_4$ unit was clearly established by HMBC correlation of Xyl$_4$ H2 with the anomeric carbon of acidic moiety. The H2 proton was TOCSY-correlated with other protons of xylose molecule and in particular COSY-correlated with anomeric proton/carbon at 4.61/102.60 ppm.

We have demonstrated that *T. neapolitana* crude homogenate is able to transfer xylan blocks higher than linear tetrasaccharide and blocks containing acidic moiety, to the aromatic (9H-fluoren-9-yl)-methanol acceptor extending the preliminary results previously reported [8]. The higher yield of product obtained with birchwood xylan with respect to 4-O-Me-glucuronoxylan as donor, is probably due to the higher distribution of acidic components in the oligosaccharidic chain of the latter. Indeed, the almost identical ratios of formed neutral/total and acidic/neutral xylosides, could confirm this view. Although the structures of the transglycosylation products agree with the mode of action of endoxylanases present in the microorganism [23], detailed information on enzymatic subsites structures is not discussed because of the presence of different β-glycosidases in crude homogenate [24]. However, the purity at anomeric position and at the interglycosidic linkages of the products obtained make them attractive for a competent analysis of the biological response with assignment of the role of acidic branched residue in aggregation phenomena and 3-D structure.

3.2. Aggregation

During structural identification, proton spectra of the trixyloside **3** and of the tetraxyloside **4** indicated a concentration-dependent self-association. The concentration study of **3** is summarized in Fig. 2 for the resonances in the regions 8.2–7.4, and 4.6–4.0 ppm, originating from the fluorenyl and carbohydrate signals, respectively. At 9.0 mM (Fig. 2D) the resonances of the fluorenyl moiety (at sites 2, 5, 4, and 3), resonating at 7.85, 7.69, 7.43 and 7.37 ppm, respectively), and methylene and methine groups of aglycone ($CH_2''O$–, CH–, and $CH_2'O$– resonating at 4.32, 4.26, and 4.12 ppm, respectively), appeared broad and scarcely resolved. As the concentration was decreased from 9.0 to 3.0 mM (Fig. 2C), the resonances were more resolved clearly showing their multiplicity, and all shift toward low field (increased chemical shift). In particular, this was noticed for the aromatic signals of the fluorenyl as well as for its methylene (at 4.32, and 4.12 ppm) and methine (at 4.26 ppm) groups. The three anomeric doublets centered around 4.4 ppm only showed a slight rearrangement of their position, the first two overlapping in a triplet. From 3.0 mM to 0.75 and 0.12 mM (Fig. 2C-B-A) no variations were observed in line shape and chemical shifts. These results are consistent with a monomeric state at low concentration for compound **3**, to become oligomeric at higher concentration (>3.0 mM). Identical results are observed for compound **4** (not shown).

Confirmation of the monomeric random coil state of **3** at 0.75 mM concentration was indeed obtained from NOESY spectra. A comparison between NOESY spectra recorded at 50, 100, 150, and 250 ms at 9.0 and 0.75 mM indicated for the highest concentration the presence of several effects, which were absent at the lower concentration. In particular, for 150- and 250-ms mixing times at high concentration we detected peaks that could most likely originate from intermolecular contacts; these peaks were absent at low concentration.

Since only one set of resonances is observed throughout the concentration range studied, this indicates that the xylosaccharides **3** and **4** associates into a symmetric oligomer or that the monomer-oligomer exchange is fast or near fast exchange on the NMR time scale. Therefore no conclusions can be inferred about the symmetry of the xylosaccharides in the aggregate. The increased line-width of fluorenyl aromatic resonances suggests for this part of the xylosaccharides a pivotal role for the aggregation. It appears that the stacking of aromatic rings (also inferred by the high field shift of the signals) may favor intermolecular interactions, and that the broadening is due to exchange between different structural arrangements, monomer-to-oligomer. It does not appear to be due to some sort of intramonomer rearrangement or exchange with solvent because the molecules are too small to give rise to internal rearrangement and, for the solvent,

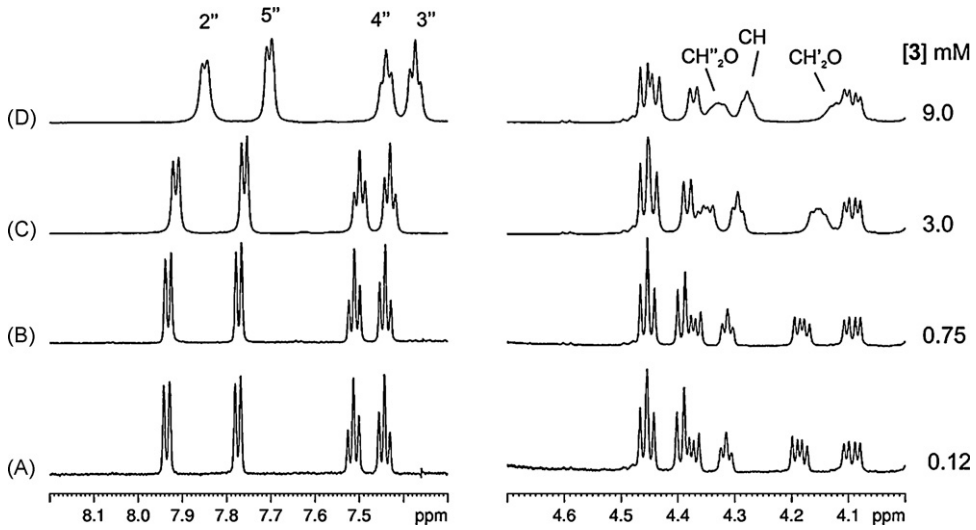

Fig. 2. ^{1}H NMR spectra of compound **3** as a function of concentration: (A) 0.12, (B) 0.75, (C) 3.0 and (D) 9.0 mM. Labels refer to fluorenyl signals resonating in the regions 8.2–7.4, and 4.6–4.0 ppm.

the resonances sharpen as the temperature is raised (data not shown).

Similar results were observed for xylosaccharide **5**, while compounds **1** and **2** gave rise to more intense effects most likely due to the reduced length of the molecules, which is expected to favor molecular packing. Indeed for these compounds suspensions in water are observed starting at 0.75 mM.

The role of MeGlcUA was investigated in compounds **6** and **7**, which differ from **3** and **4**, respectively, for the addition of the acidic moiety. We did not detect concentration dependence of the ^{1}H NMR spectra for **6** (Fig. 1) and **7** at all concentration investigated. These data suggest that the presence of the MeGlcUA prevents aggregation so as to disfavor intermolecular interactions to form oligomer. Intramolecular interactions were uncovered by investigating the solution structure of **6** (see below).

3.3. Cell proliferation assay

The effects of polyxylosylation and presence or absence of MeGlcUA on the activity of compounds **1**–**7** (Scheme 1) were assayed on human epithelial EFO 27 ovarian cancer cells, aiming at investigating the ability of products to reduce cell proliferation (Table 2). The measured IC_{50} (μM) values indicated that for compounds **1**–**5**, which all lack MeGlcUA, the IC_{50} increases together with the lengthening of the xylose chain. That is, a longer chain brings about an immediate reduction of the antiproliferative activity, turning **2**–**5** into inactive compounds while compound **1** preserves an IC_{50} comparable to the most active xylosaccharides **6** and **7** (204.4 and 218.6 μM, respectively) which are the highest ones. The striking difference of activity observed comparing **6** and **3**, and **7** and **4** (Table 2), should be linked to the presence/absence of MeGlcUA, and possibly to the conformation taken up by the molecule in the presence/absence of MeGlcUA.

Table 2
Effect of polyxylosides of Scheme 1 on EFO[a] cells growth.

Compound	IC_{50} (μM)[b]
1	304.0 ± 5.5
2	>434.3 ± 7.8
3	[c]
4	[c]
5	[c]
6	204.4 ± 1.2
7	218.6 ± 0.9

[a] Human ovary adenocarcinoma (EFO 27) cell lines.
[b] Data are reported as mean ± S.E. of IC_{50} values (μM) calculated from two independent experiments.
[c] No significant activity was observed.

3.4. Solution structure of the acidic xylotetrasaccharide **6**

The lack of aggregation for compounds **6** and **7** (see above) indicated a possible role for MeGlcUA in preventing aggregation so as to disfavor intermolecular interactions to form oligomers. Because **6** and **7** gave similar spectra, the solution structure will be detailed for compound **6** in order to uncover these interactions.

Its 3D structure was studied by resorting to NOESY experiments (mixing times 50, 100, 150, 250, and 350 ms), and calculations.

Surprisingly, even at 50 ms we detected 24 intra- and 10 inter-residue effects, which increased upon mixing-time lengthening: 26 and 12 at 100 ms, 33 and 17 at 150 ms, 35 and 17 at 250 ms, to reach 41 and 25 at 350 ms. Interestingly, at 150 ms mixing time, some of these intra-residue contacts are among 1,3-diaxial protons within each sugar. This suggests that all the sugar rings in the molecule possess a $^4C_1$ chair conformation. This observation was further inferred by the analysis of the proton coupling constants measured for the protons belonging to the sugar rings: *ca.* 9 Hz for the trans-diaxial protons and *ca.* 4 Hz for the coupling constants involving equatorial hydrogens. Instead, some of the inter-residue contacts are interglycosidic NOE contacts, suggesting that the molecule takes up a well-defined rigid conformation. In particular, at 150 ms mixing time, NOE contacts between consecutive sugars suggested the reciprocal position of ring pairs. Furthermore, we also detected cross-peaks between protons located on alternate rings: namely, MeGlcUA H1 with the Xyl_2 (middle xylose) H5; MeGlcUA H3 (3.76 ppm) and H5 (4.30 ppm) correlated both with H5′ (3.43 ppm) of Xyl_2; -OMe residue of MeGlcUA showed a NOE-effect with Xyl_1 (internal xylose) H1 and Xyl_3 (external xylose) H1. We also observed a NOE-effect between MeGlcUA H4 and H5′ of aromatic residue (Fig. 3). Furthermore, at 250 ms mixing time, the H4 of the MeGlcUA moiety exhibited correlation with Xyl_1 H3, and Xyl_1 H5 with Xyl_2 H5′. All these connectivities imply that in **6** the aromatic ring folds toward the carbohydrate chain. In particular, the long-range contacts forced the molecule in a non-planar arrangement, being the fluorenyl bent toward the MeGlcUA.

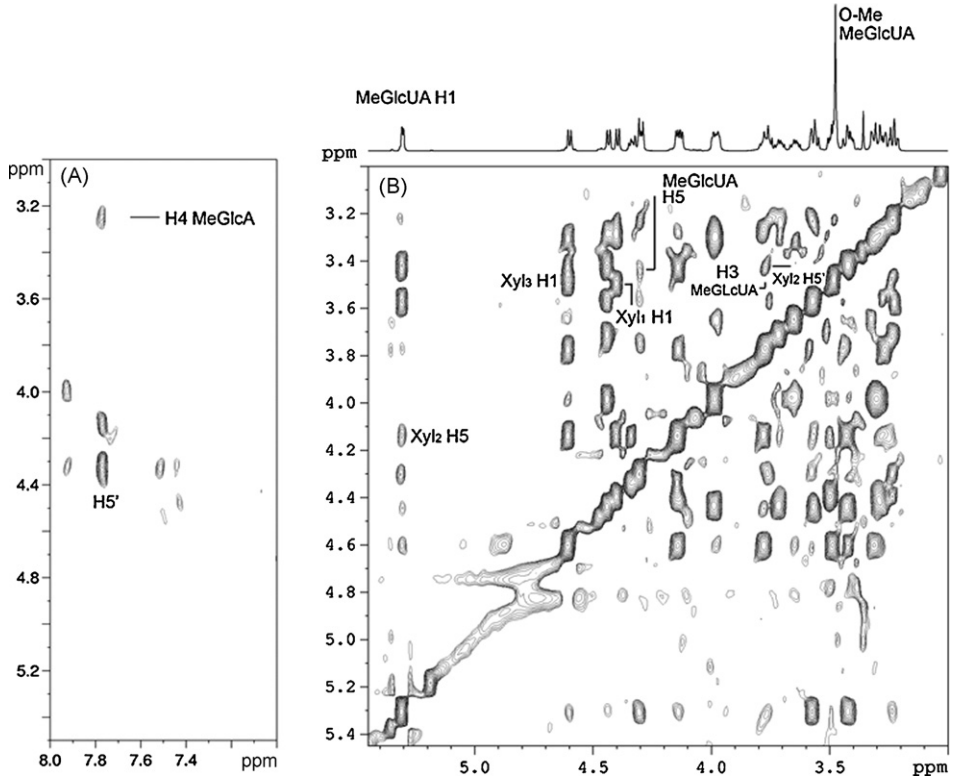

Fig. 3. NOESY spectrum (τ_m = 250 ms) of compound **6** showing (A) cross-peaks between H5′ of the aglycone with the H4 of the MeGlcUA moiety, and (B) MeGlcUA H1 with the Xyl_2 H5. MeGlcUA H3 and H5 correlated both with H5′ of Xyl_2 and –OMe residue of MeGlcUA showed a NOE-effect with Xyl_1 H1 and Xyl_3 H1.

As stated above, **6** was investigated at pH 3.7 and 6.8. At acidic pH, when the MeGlcUA is protonated, the NOE pattern (not shown) is the same as that observed at pH 6.8, implying that any structural effects induced by protonation/deprotonation of MeGlcUA must be small.

In order to obtain the three-dimensional structure of **6** at atomic level, an estimation of proton–proton distances has been retrieved from cross-peak intensities in 2D NOESY experiment acquired with mixing time of 150 ms. Pseudo-atoms were introduced where needed. A total of 38 distances constraints were used for the calculations (Table 3). Moreover, 11 dihedral angle constraints (that correspond to $^3J_{HH}$ coupling constants that yielded only two real roots when solving Karplus equation) were also used. Therefore, three-dimensional structures of **6** which satisfy NOEs and dihedral angle constraints were constructed by restrained simulated annealing calculations. An initial structure of **6** was constructed and minimized, in order to eliminate any possible source of initial bias in conformation. Restrained simulations were carried out *in vacuo* for 12.5 ns using the Consistent Valence Force Field (CVFF) as implemented in Discover software (Accelrys, San Diego, USA). The initial temperature was set at 1000 K. Thereafter, the temperature was decreased stepwise to 250 K. The final step was to energy-minimize and refine the structures obtained by using the steepest descent and the quasi-Newton–Raphson (VA09A) algorithms. A total of 50 structures were generated. The 10 structures with lowest energies were selected. It was possible to obtain an excellent superimposition of the 10 structures with RMSD values of 0.14 ± 0.21 for heavy atoms (Fig. 4A). The structures were also energy minimized without experimental restraints, and the results are shown in Fig. 4B. As expected the superimposition is slightly worst than that obtained with restraints, but the found RMSD values of 0.42 ± 0.15 warrants the quality of the structure confirming that the calculated structure is stable and not induced by NMR restraints.

Table 3
NMR-derived experimental constraints and structure statistics of the best 10 structures.

Experimental constraints	
Total NOEs	38
Dihedral angle constraints	11
CVFF energy (kcal mol^{-1}) of the minimized structures	
Total	142.071 ± 0.0985
Non-bond	68.705 ± 0.0424
Restraint	0.676 ± 0.0039
NOEs violations	
Number >0.1 Å	1 ± 0.0
Maximum (Å)	0.228 ± 0.0026
Sum (Å)	0.619 ± 0.004
Average violation (Å)	0.016
r.m.s. deviations from the mean structure (Å)	
All heavy atoms	0.14 ± 0.21

As shown, the presence of the MeGlcUA ring in compounds **6** and **7** hampers aggregation as we did not detect concentration dependence of the ^{1}H NMR spectra for both acidic xylosaccharides at all concentrations investigated. Interestingly, MeGlcUA moiety, along with the external and middle xyloses, adopts in solution a hairpin-shaped conformation, generating a non-planar arrangement of the molecule. This spatial arrangement seems to be favored both by the formation of an H-bond (observed in 9 calculated structures out of 10) between OH in position 2 of the MeGlcUA moiety and the oxygen linking Xyl_1–Xyl_2, and by the favorable hydrophobic interaction among the methyl ether of MeGlcUA, the hydrophobic side of Xyl_1 and the aglycon methylene. Furthermore the orientation of the aromatic ring and the non-planar conformation of the sugar moieties prevent, respectively, an efficient π-stacking [25] to initiate aggregation and the following packing of the xylose chains, therefore avoiding aggregation for **6** and **7**.

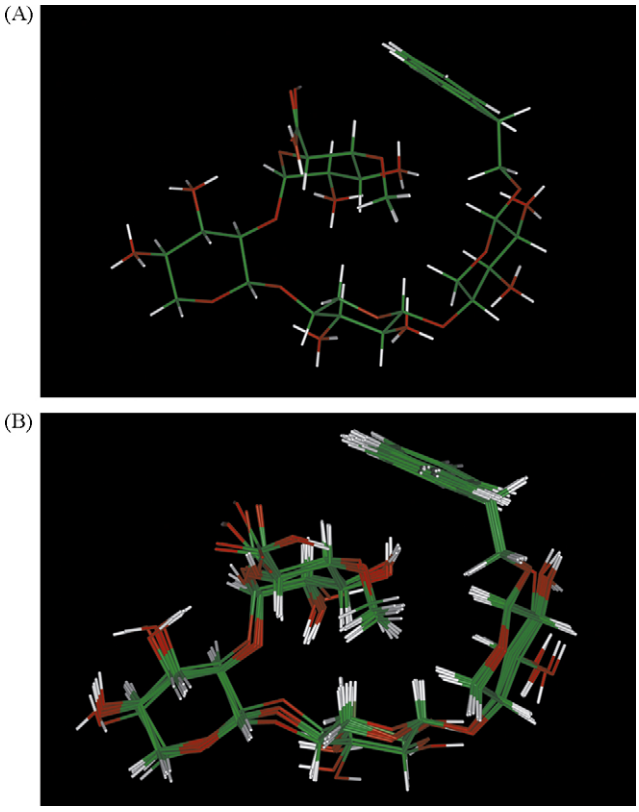

Fig. 4. Superimposition of the best 10 structures of **6** after restrained (A) and unrestrained (B) minimization. The molecules are depicted in colored "stick" (carbons, green; oxygens, red; hydrogens, white) (For interpretation of the references to color in this figure legend, the reader is referred to the web version of the article.).

All these results suggest a structure–activity relationship identifying the role of 4-O-methyl glucuronic acid in regulating aggregation of these molecules. This moiety was recognized to be heavily involved in the stability of conformations. An immediate reduction of the anti-proliferative activity was shown increasing the number of xylose units while it was observed that polyxylosylation in compounds **1**–**5** caused antiviral activity to increase as tested using human peripheral blood mononuclear cells [7].

Since bioavailability together with therapeutic activity is an important issue of biopharmaceuticals, further studies on variously structured biological systems (whole cells, free systems, receptors) are necessary to correlate aggregation with biological activities.

Acknowledgements

The financial support is provided by CNR funding to Istituto di Chimica Biomolecolare and by Progetto F.I.S.R. no. 1756. We thank Eduardo Pagnotta and Emilio P. Castelluccio (ICB-CNR, Pozzuoli) for the skillful lab assistance and computer maintenance, respectively.

This paper is dedicated to the memory of Prof. R.A. Nicolaus.

References

[1] A. Trincone, A. Giordano, Curr. Org. Chem. 10 (2006) 1163–1193.
[2] N. Kulkarni, A. Shendye, M. Rao, FEMS Microbiol. Rev. 23 (1999) 411–456.
[3] S. Matsumura, K. Sakiyama, K. Toshima, Biotechnol. Lett. 21 (1999) 17–22.
[4] P. Christakopoulos, P. Katapodis, E. Kalogeris, D. Kekos, B.J. Macris, H. Stamatis, H. Skaltsa, Int. J. Biol. Macromol. 31 (2003) 171–175.
[5] M. Hashi, T. Takeshita, Agric. Biol. Chem. 43 (1979) 961–964.
[6] A. Ebringerova, A. Kardosova, Z. Hromadkova, A. Malovikova, V. Hribalova, Int. J. Biol. Macromol. 30 (2002) 1–6.
[7] A. Tramice, A. Arena, A. De Gregorio, R. Ottanà, R. Maccari, B. Pavone, N. Arena, D. Iannello, M.G. Vigorita, A. Trincone, ChemMedChem 9 (2008) 1419–1426.
[8] A. Tramice, E. Pagnotta, I. Romano, A. Gambacorta, A. Trincone, J. Mol. Catal. B-Enz. 47 (2007) 21–27.
[9] H. Schellekens, Nat. Rev. Drug Discov. 1 (2002) 457–462.
[10] A. Braun, L. Kwee, M.A. Labow, J. Alsenz Pharmacol. Res. 14 (1997) 1472–1478.
[11] L. Curatolo, B. Valsasina, C. Caccia, G.L. Raimondi, G. Orsini, A. Bianchetti, Cytokine 9 (1997) 734–739.
[12] S. Lesné, M.T. Koh, L. Kotilinek, R. Kayed, C.G. Glabe, A. Yang, M. Gallagher, K.H. Ashe, Nature 440 (2006) 352–357.
[13] L. Braunschweiler, R.R. Ernst, J. Magn. Reson. 53 (1983) 521–528.
[14] C. Griesinger, G. Otting, K. Wüthrich, R.R. Ernst, J. Am. Chem. Soc. 110 (1988) 7870–7872.
[15] J. Jeener, B.H. Meier, P. Bachmann, R.R. Ernst, J. Chem. Phys. 71 (1979) 4546–4553.
[16] L.E. Kay, P. Keifer, T. Saarinen, J. Am. Chem. Soc. 114 (1992) 10663–10665.
[17] A. Bax, M.F. Summers, J. Am. Chem. Soc. 108 (1986) 2093–2094.
[18] M. Karplus, J. Am. Chem. Soc. 82 (1960) 4431–4432.
[19] A.C. Wang, A. Bax, J. Am. Chem. Soc. 118 (1996) 2483–2494.
[20] S.J. Weiner, P.A. Kollman, D.A. Case, U.C. Singh, C. Ghio, G. Alagona, S. Profeta, P.J. Weiner, J. Am. Chem. Soc. 106 (1984) 765–784.
[21] O. Jardetzky, Biochim. Biophys. Acta 621 (1980) 227–232.
[22] A. Teleman, V. Harjunpää, M. Tenkanen, J. Buchert, T. Hausalo, T. Drakenberg, T. Vuorinen, Carbohyd. Res. 272 (1995) 55–71.
[23] A. Sunna, J. Pulse, G. Antranikian, Comp. Biochem. Physiol. 118 (1997) 453–461.
[24] V. Zverlov, K. Piotukh, O. Dakhova, G. Velikodvorskaya, R. Borriss, Appl. Microbiol. Biotechnol. 45 (1996) 245–247.
[25] E.A. Meyer, R.K. Castellano, F. Diederich, Angew. Chem. Int. Ed. Engl. 42 (2003) 1210–1250 (Erratum in: Angew. Chem. Int. Ed. Engl. 42 (2003) 4120).